


Summary of “Physics of Photocathodes for Photoinjectors” workshop BNL, October 3-5, 2023

Luca Cultrera

EWPPA – workshop – HZDR, September 17-19, 2024

    @BrookhavenLab

Special Thanks

Local Organizing Committee

- L. Cultrera (co-Chair)
- M. Gaowei (co-Chair)
- S. Capp

Support staff

- C. Weaver
- D. Basozmen

Scientific Committee

- Luca Cultrera
- Oksana Chubenko
- Dimitre Dimitrov
- Mengjia Gaowei
- Carlos Hernandez-Garcia
- Kevin Jensen
- Siddharth Karkare
- Jared Maxson
- Nathan Moody
- Pietro Musumeci
- John Smedley
- Marcy Stutzman
- Theodore Vecchione

P3 workshop 2023, BNL



75 Registered participants



7 sessions, 37 talks



15 posters

P3 workshop 2023, BNL



7 plenary sessions

- **Introductory session**
- **High charge - High average current**
- **Free Electron Laser (two sessions)**
- **Theory (two sessions)**
- **Novel concepts (two sessions)**
- **Ultrafast Diffraction and microscopy**
- **Spin polarized sources**

I will try to give an objective and comprehensive summary

Talks are uploaded to the following indico website

[Photocathode Physics for Photoinjectors Workshop \(3-October 5, 2023\) · Indico \(bnl.gov\)](#)

Introductory session



EWPA 2022 Highlights

D. Sertore
INFN Milan – LASA
Lee Jones (STFC, DL), On behalf of the EWPA 2022 Organizing Committee

ERL in European Strategy for Particle Accelerator

Accelerator R&D Roadmap and its impact on photocathode research

- New accelerator roadmap emphasise interest to further development of **Energy Recovery Linacs (ERL) as high efficiency sustainable accelerator facilities**.
- High average current, in **100 mA range**, electron injectors are one of the most critical components of ERLs and additional efforts should be concentrated on further development of the injectors.
- Major efforts should be concentrated on the following:
 - Optimisation technology of existing photocathode materials**
 - Development new photocathode materials which could operate with existing laser system**
 - Design photocathode plug which may be compatible with different types of the guns**
- Development of laser systems which would allow for delivery required current with UV photocathodes
- Development of gun technologies which would allow for providing beams compatible with existing accelerator structures without excessive bunching schemes. Potential to reach this goal have.
 - High field QWR SRF gun**
 - High field QWR NCRF gun**
 - Elliptical cavity SRF gun**
- There is no operational injector which can demonstrate **100 mA** of polarised current: Limited by photocathode lifetime
- Potential to deliver this current (if GaAs lifetime by activation with Cs-alkali metal layer is successful),
 - DC photocathode guns
 - SRF photocathode guns



Boris Militsyn
STFC Daresbury Laboratory, UK

Electron Sources for Particle Accelerators

YINE SUN
Advanced Photon Source
Argonne National Lab.

Oct. 3, 2023
Photocathode Physics for Photoinjectors Workshop
Stony Brook, New York



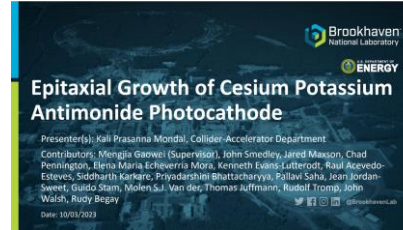
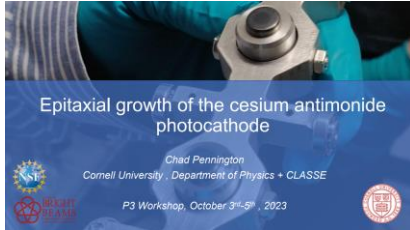
April 2023: e⁺ Source Roadmap Working Group Report

<https://indico.fnal.gov/event/59123/>

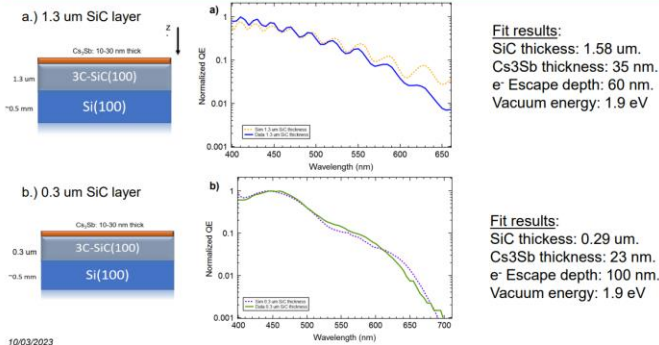
Year	Near-term (<5 years)	Mid-term (5~10 years)	Long-term (10~20 years)
e ⁻ Cathode	Reliable high-P GaAs supply chain	Cryogenic temperatures and very high fields operation	
	Robust photocathodes in DC guns (20mA pol. and 100 mA unpol.)		
	Photocathodes with 1% QE and 30 meV MTEs	Photocathodes with 1% QE and 5 meV MTEs	
	Continue to explore new and promising photocathodes (robust surfaces, nano-structures, higher QE and polarization)		
e ⁻ Gun	DC gun beam ~1-10 mA polarized	10 ⁻¹⁴ Torr vacuum for long GaAs lifetime	DC gun beam 10~20 mA polarized
	NCRF: cryo gun at 250 MV/m; x-band gun, CW and Low Frequency rf gun		
	Polarized GaAs in an SRF photogun	SCRF gun 50 MV/m	
e ⁻ Injector	Control laser profile, limit nonlinear SC induced emittance growth: beer can (mid); elliptical (far)		
	NCRF, SRF accelerating cavities: fully RF symmetrized fields to eliminate emittance growth to 10% (near), 1% (mid), 0.1% (far)		
	Partition phase space: RFBT+EXX for damping ring free (mid), linear LPS (long)		
	High Charge Drive Bunch Trains: charge-balanced, equal energy bunches duration 5-25 nsec.		
e ⁺ polarized	SC undulators	Collider-class polarized e ⁺ source	
	Compton-based sources - high flux circularly polarized gamma-rays R&D		
	Bremsstrahlung polarized positron source development		
e ⁺ unpolarized	Targets for high intensity		
	Capture and acceleration sections		
	Compact sources for accelerator and ultrafast science (also polarized)		
	10 ⁻¹⁴ Torr vacuum for long GaAs lifetime	Routine 10's mA GaAs beams	

Photocathode Physics for Photoinjectors Workshop
Sun 10/3/2023 Yine

High Charge / High Average Current

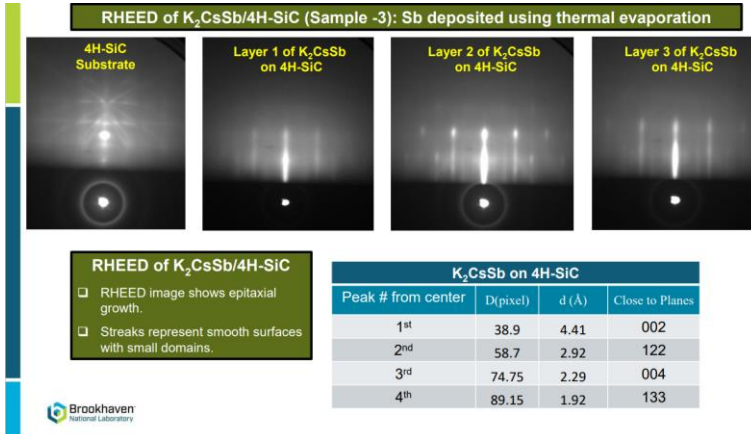


Optical interference in the cathode substrate



10/03/2023

26

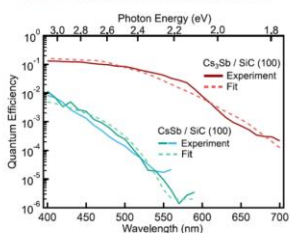


Brookhaven
National Laboratory

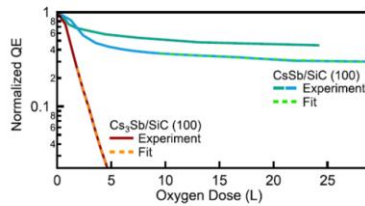
26

An alternate stoichiometry: Cs_1Sb_1

- A visible photocathode with threshold near 570 nm and percent level QE at 400 nm.



- Highly resistant to oxidation.
- Survives over an order of magnitude times longer than Cs_3Sb at an O_2 partial pressure of 5×10^{-8} Torr.

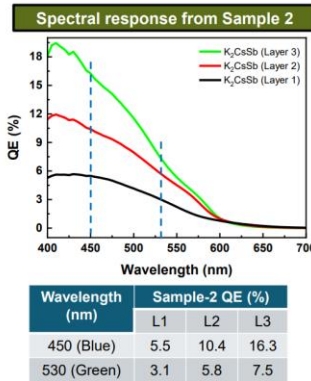


- Photoemission threshold lies between Cs_3Te and other alkali antimonides.

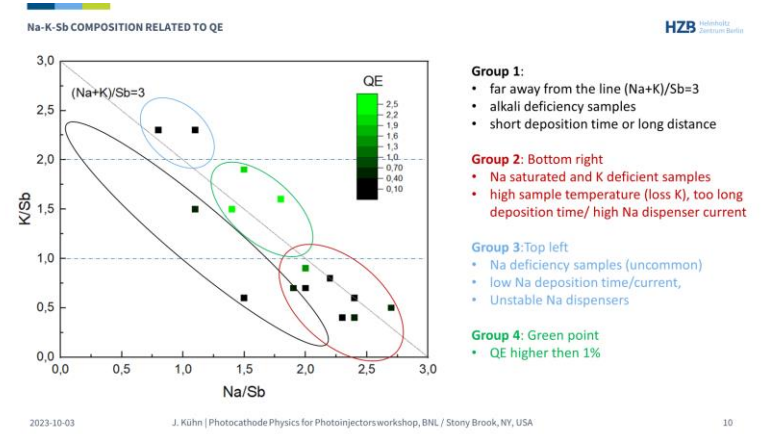
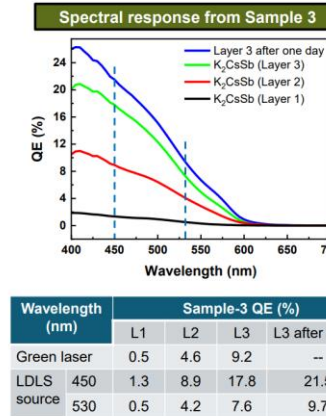
C.T. Parzyk, C.A. Pennington et al. "Atomically smooth films of CsSb: a chemically robust visible light photocathode" arXiv:2305.19553

10/03/2023

30



Brookhaven
National Laboratory



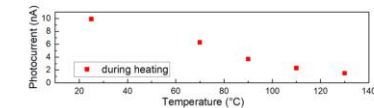
2023-10-03

J. Kühn | Photocathode Physics for Photoinjectors workshop, BNL / Stony Brook, NY, USA

10

ROBUSTNESS INVESTIGATIONS ON Na-K-Sb PHOTOCATHODES

Thermal stability study of Na-K-Sb: 4 heating cycles up to 130°C, XPS data taken at RT after 24h heating



Chemical composition change after heating					
Day	Na	K	Sb	(Na+K)/Sb	QE (%)
WH17	1.6	1.9	1.0	3.5	1.1
WH17	1.5	1.9	1.0	3.4	1.1
WH17	1.6	1.8	1.0	3.4	1.1
WH17	1.8	1.7	1.0	3.5	0.8
WH17	1.7	1.4	1.0	3.1	0.5

2023-10-03

J. Kühn | Photocathode Physics for Photoinjectors workshop, BNL / Stony Brook, NY, USA

14

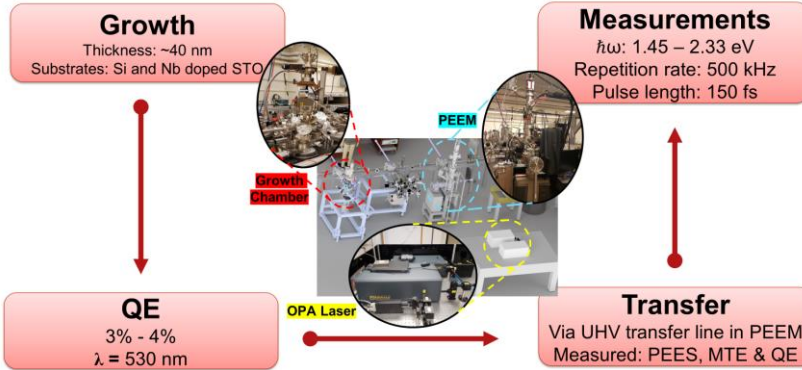
High Charge / High Average Current



Demonstration of Thermal Limit to Mean Transverse Energy from Cesium Antimonide Photocathode
Alimohammed Kachwala
Arizona State University



Experiment



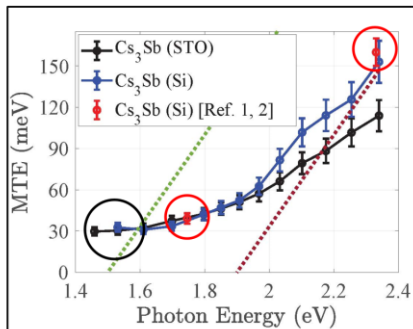
8/6/2024

akachwal@asu.edu

10



Mean Transverse Energy



- At $\hbar\omega = 1.5$ eV, MTE = 30 meV (~25 meV at 300 K)
- At $\hbar\omega = 1.8$ eV, MTE = 40 meV and at $\hbar\omega = 2.3$ eV, MTE = 150 meV (comparable to previously reported values)
- The dotted line is the plot for (excess energy)/3 considering $\Phi = 1.5$ eV (green) and $\Phi = 1.9$ eV (brown)
- MTE doesn't scale as $1/3^{\text{rd}}$ of excess energy (Scattering before emission)

1) Physical Review Special Topics-Accelerators and Beams 18.11 (2015): 113401.
2) Applied Physics Letters 99.15 (2011):

8/6/2024

akachwal@asu.edu

14

Development of Multialkali antimonides photocathodes for high-brightness photoinjectors

Event: P3 Photocathode Workshop, October 3rd - 5th, 2023, New York, USA

Speaker:
Sandeep Kumar Mohanty

Co-authors:
M. Kowalewski, A. Cappel, F. Steinhilber
DESY, Zeuthen, Germany
D. Soriano, L. Minello, G. Guenther-Rocco
INFN-LASA, Segrate, Italy and Universita degli Studi di Milano

Contents:

- Multi-alkali antimonides photocathodes development
- Why the Optical properties are important?
- Experimental results (Cathode 1 & 2)
- Density Functional Theory (DFT) study (K₃Sb, K₂CsSb)
- Comparison with experimental results
- Summary & Future plan



P3 Photocathode Workshop 2023, October 3rd - 5th, 2023

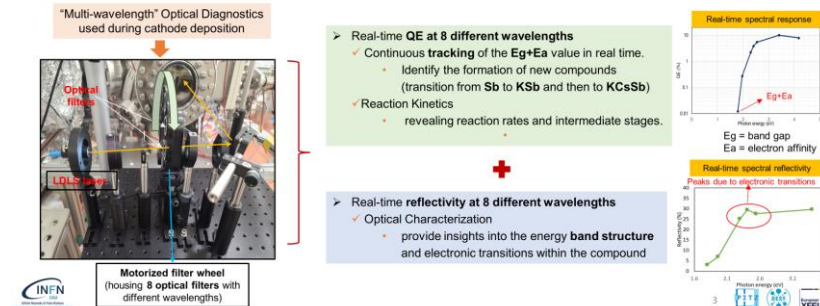


Multi-alkali antimonides photocathodes development

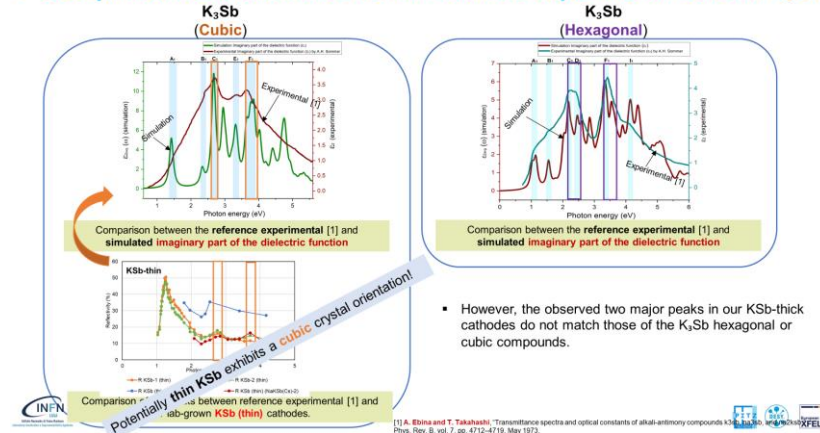
- To improve + optimize cathode recipe:

- Two new cathodes grown in the new "production" system.
 - One thick (Sb = 10 nm) (#137.2)
 - One thin (Sb = 5 nm) (#137.3)

- To understand the evolving photocathode structure during and after deposition, a "multi-wavelength" diagnostic setup is utilized.



Comparison between the DFT Simulation and Experimental Data for K₃Sb



- However, the observed two major peaks in our K₃Sb-thin cathodes do not match those of the K₃Sb hexagonal or cubic compounds.

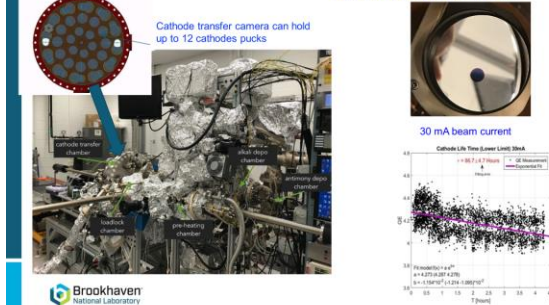
[1] A. Bina and T. Takahashi, "Transmittance spectra and optical constants of alkali-antimony compounds K₃Sb, K₂CsSb, and K₃Bi," Phys. Rev. B, vol. 7, pp. 4712-4719, May 1973.



2) Photocathodes production

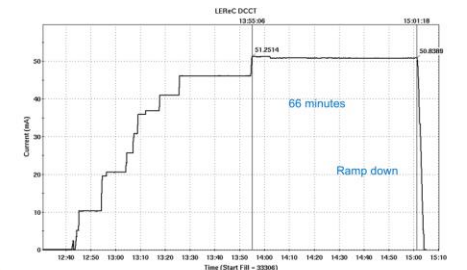
- To support 24/7 operations, cathode production and exchange systems were developed which include two cathode deposition systems, three multi-cathode (up to 12 cathodes) vacuum suites and a mechanism allowing for cathode exchange in RHIC tunnel in about 1 hour.
- DC gun with high QE cathodes and stable laser provided reliable beam operation during 2019 - 2021

Off center by 4 mm small active area (6mm), used at the end of 2018 and 2019-2022.



3) Higher Current Test

- 320kV: if the HVPS Faults are not caused by the voltage, could try 350kV later.
- 66 minutes: The current was ramped down prior to next polarization measurements in RHIC which typically results in high losses in the location of the Gun.
- 50 mA: limited by the injection dump power (25kW);



20

Free Electron laser



R&D of Very High Frequency (VHF) gun for
SHINE project at Tsinghua University

Yingchao Du

Department of Engineering Physics, Tsinghua University
Beijing, China, 100084

dych@tsinghua.edu.cn



PROGRESS REPORT ON AN X-BAND ULTRA-HIGH GRADIENT PHOTOINJECTOR



GONGXIAOHUI CHEN
on behalf of joint efforts from ANA, Euclid Techlabs and NIU

CHICAGO ARGONNE ENERGY

10/03/2023



Successful operation of K_2CsSb photocathode in DC-SRF-II gun

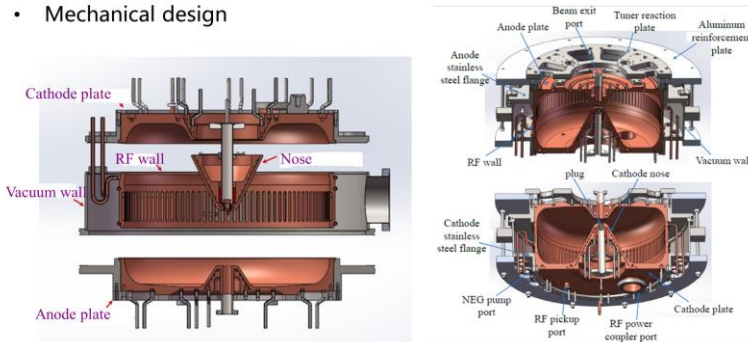
XIE Huamu on behalf the SRF team at PKU
Oct3-5, 2023
Photocathode Physics for Photoinjectors Workshop

北京大学物理学院加速器实验室



VHF gun RF design and optimization

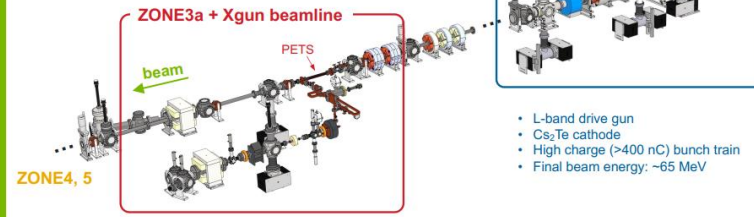
Mechanical design



14

INTRODUCTION TO AWA DRIVE BEAMLINE

- Fully re-configurable
- Currently have a metallic Power Extraction and Transfer Structure (PETS) installed

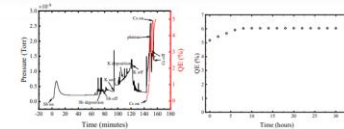


- L-band drive gun
- Cs_2Te cathode
- High charge (>400 nC) bunch train
- Final beam energy: ~65 MeV

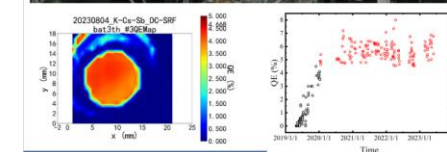
CHICAGO ARGONNE ENERGY

7

K_2CsSb photocathode deposition system



"Fast Cessation" sequential deposition recipe, the total activation time cost less than 10 min. The QE keeps growing in the following days after activation.



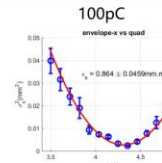
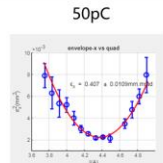
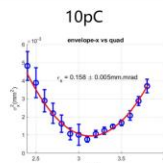
Photocathode grown by co-evaporation method



Beam testing

Emittance measurement and optimization (preliminary results)

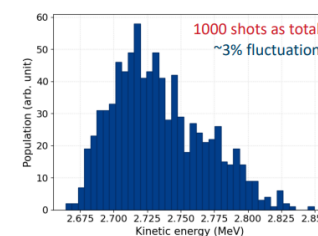
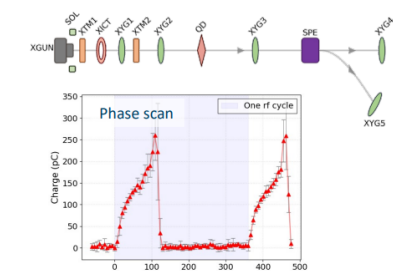
Bunch charge	Projected emittance (95%) ($\mu m \cdot rad$)	Slice emittance (95%) ($\mu m \cdot rad$)	Bunch length (mm rms)
10 pC	0.16	0.15	0.49
50 pC	0.41	0.38	1.15
100 pC	0.85	0.72	1.44



24

BEAM ENERGY CHARACTERIZATION

1st beam test



- Xgun phase scan @340 MV/m
- Evidence of strong Schottky effect

- Energy measured by the spectrometer dipole
- ~3% fluctuation, likely due to the drive charge instability and laser RF phase jitter in the drive linac.
- Max achieved gradient is 388 MV/m from the beam energy measurement

CHICAGO ARGONNE ENERGY

10

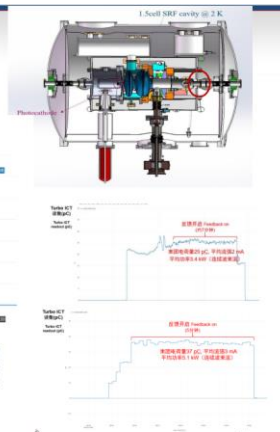
High current operation

CW operation at high average current---1 mA



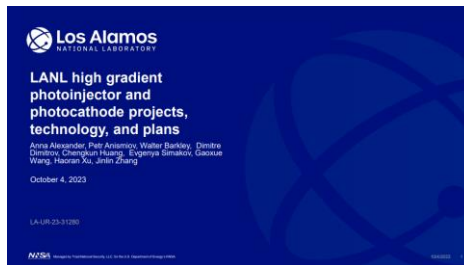
2~3 mA CW average current (12~40 pC, 81.25 MHz) also achieved in DC-SRF-II gun, the main limitation is the heat induced SC cavity quench from the beam tube connected to the SC cavity.

For more details, please contact: huangs@pku.edu.cn



10

Free Electron laser



Some of the Photocathode Science at SLAC

2023 Photocathode Physics for Photoinjectors Workshop

Theodore Vecchieme
October 4, 2023



S-band photocathode based injector plan for Korea-4GSR

2023-10-4

Chang-Ri Min
on behalf of Korea-4GSR linac group
Pohang Accelerator Laboratory

Special thanks to
-4GSR linac advisory committee, Hiroshi Matsumoto (KEK), Takahiro Inagaki (RIKEN Spring-8 Center), John Smedley (SLAC)
-MOGA simulation, Chamei Kim, Chong Shik Park, Eun-San Kim, Seung Hwan Shin, Seong Hye Park at Korea Ulsan



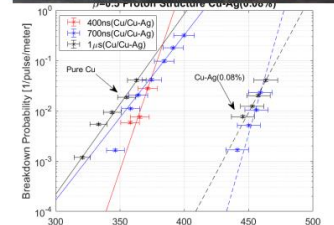
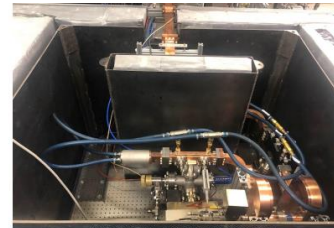
PAL POHANG ACCELERATOR LABORATORY

Carie: high gradient photoinjector capability

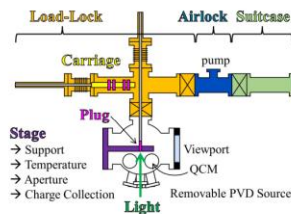
- Goal: demonstrate operation of high QE cathodes in a high-gradient RF injector

Why?

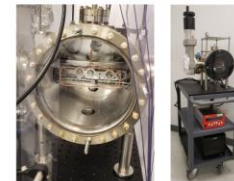
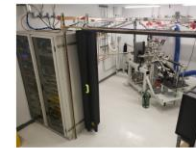
- ICS 44 keV xray source
- UED



LCLS-II Photocathode Deposition System

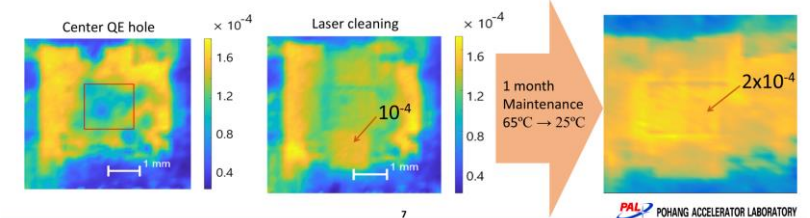


- System has four physical vapor deposition sources that are reconfigurable to produce different materials following either sequential or co-deposition recipes
- Load-Lock, Airlock and Suitcase are maintained "particle free"
- Initial QE of Cs₂Te photocathodes at 258 nm is 5-15%, with > 10% typical
- Cs₂Te QE is stable for months in a "clean" suitcase



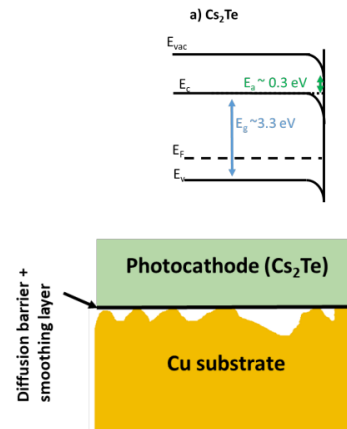
PAL-XFEL s-band photocathode gun and injector

- Maintaining the normalized emittance at 135 MeV
 - Average 0.4 u at 250 pC (variations between 0.35~0.45u)
- QE at 253 nm, 1~2x10⁻⁴, Vacuum 2x10⁻¹¹ mbar
 - Twice laser cleaning since 2016 and 2022,
 - Low surface damage using ~300 ps long IR laser cleaning
 - Half a day cleaning and operation right away



High gradient photocathode design:

- High bandgap + high(er) Ea
- Ultrathin cathodes
- Heterostructures?
- Lossy/imperfect preferred?
- Does photoemission facilitate breakdown?
- What happens to the injector when photocathodes break down?



SLAC's Grand SRF Photocathode Challenge

We have $\epsilon_s = 0.4 \mu\text{m}$ at 100 pC, 1 mm, 100 MeV (in theory)
We want $\epsilon_s < 0.1 \mu\text{m}$ at 100 pC, 1 mm, 100 MeV

Intrinsic emittance
 $\epsilon_{int} \approx 0.5 \mu\text{m/mm now}$
 $\epsilon_{int} \approx 0.3 \mu\text{m/mm future}$
 $\epsilon_{int} \approx 0.2 \mu\text{m/mm eventually}$

Dark current
 $< 1 \mu\text{A}$

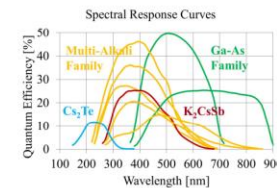
Quantum Efficiency
QE drops near threshold
QE drops with temperature

Temporal Response
 $< 50 \text{ ps}$, bunched downstream to $< 1 \text{ ps}$
 $< 1 \text{ ps}$ at the photocathode is not necessary

1/e Lifetime
 $> 1 \text{ week}$ (operational issue)

Photocathode must also not generate particles or contaminate the cavity

Operate near threshold for emission
Operate at low temperature
Reduce surface roughness
Increase chemical uniformity



Motohiro Suyama, Hamamatsu

Challenge: Which to use?

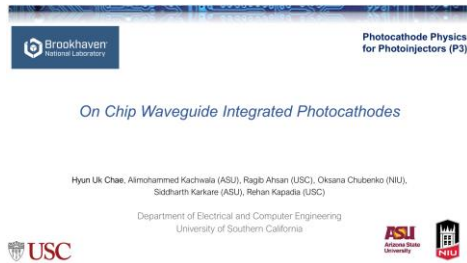
Conventional: Cs₂Sb
More exotic: Cs₂Sb:Na₃KSb
Novel: Na₂O

photocathode vs. thermionic gun

	S-band photocathode	Thermionic (DC or RF)
Emittance	O	Δ
Complexity	Δ or O with simpler laser	Δ
Clean well defined bunch	O	Δ

- Low emittance provides headroom for injection and readiness for the lower emittance storage ring upgrade
- Higher QE is preferred, then low power laser is easy to handle, more flexible to bunch patterns
- Transform-limited laser pulses ensure the well-defined bunch profile

Novel concepts

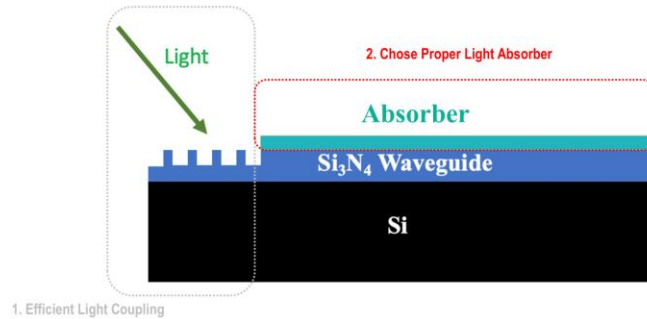


Ab initio Study of 2D Materials as Photocathode Capping Layers and Potential Photocathodes

Photocathode Physics for Photoinjectors



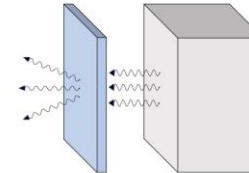
Key factors of designing good Photocathode



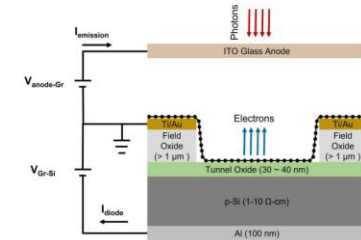
Why Scattering States are Important

Electron Transparency and Reflectivity

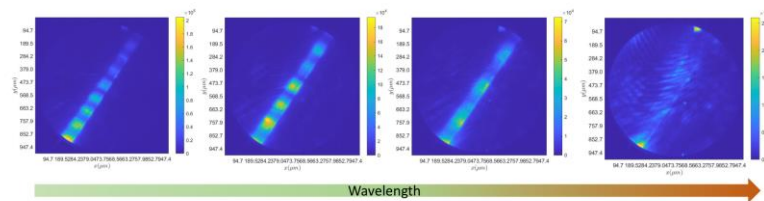
- Mean-transverse energy (MTE) and quantum efficiency (QE) are modulated by capping layers
- We need electron transparency and reflectivity
- Transmission and reflection can be taken directly from scattering states



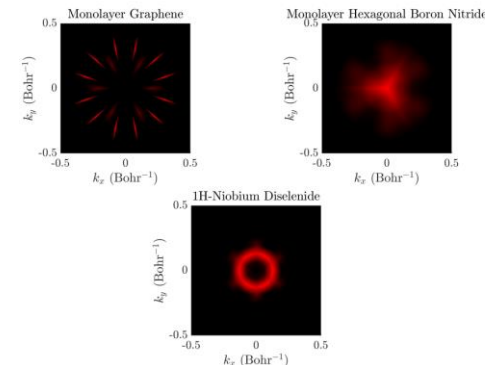
Electronically Tunable NEA Photocathode



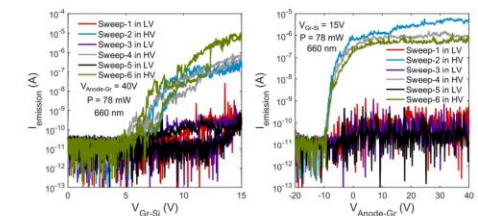
Wavelength Dependent Photoemission



Results: Summary of Photoemission

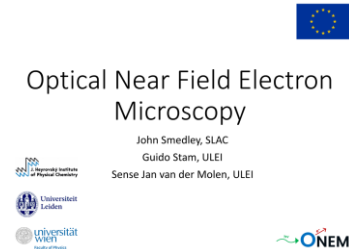


Stability at higher vacuum pressures

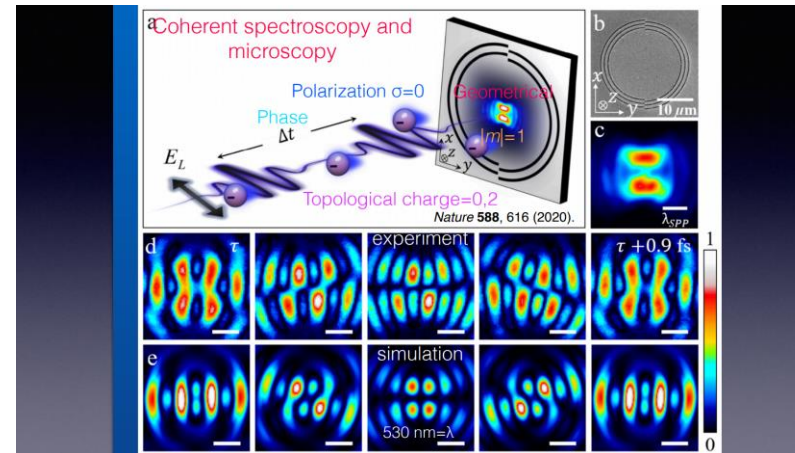
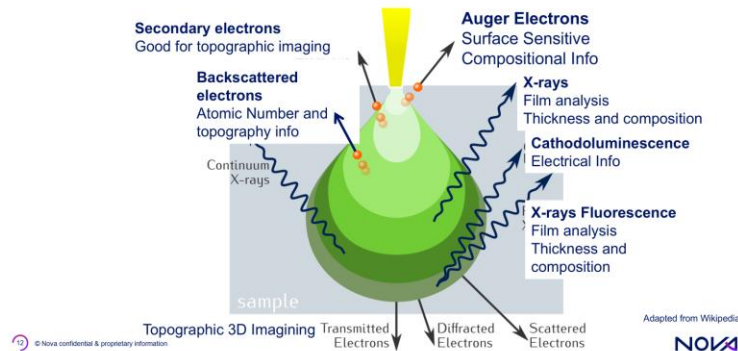


- The period of the pattern increases as we go from $\lambda = 520$ nm to $\lambda = 532$ nm.
- These transverse patterns are formed due to interference between these co-propagating modes thereby generating beating patterns with significant evanescent intensities that cause the electron emission.

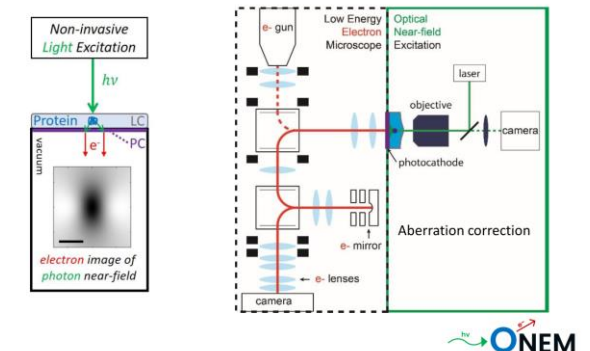
Novel concepts



Electron Beams Have Many Capabilities to Address Many of the Needs For Metrology and Inspection



Positioning ONEM in LEEM



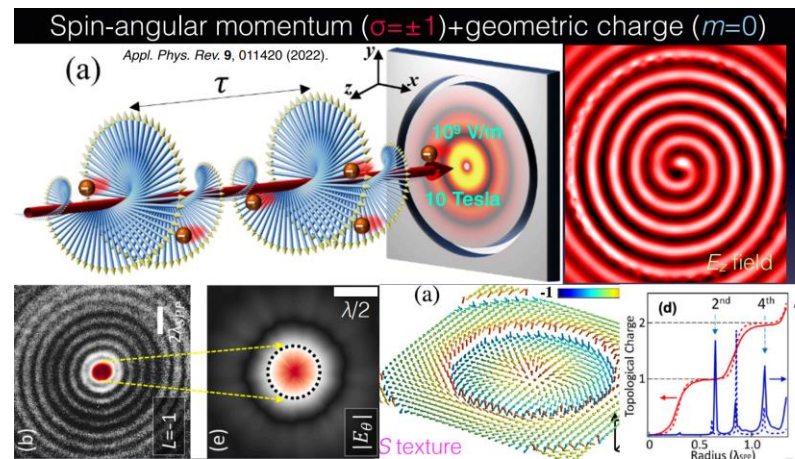
E-Beam Source Requirements for Metrology

Electron Source

- ✓ Energy Spread ≤ 0.3 eV
- ✓ High Brightness $> 10^8$ A / (V m² sr)
- ✓ Focus to high current densities
- ✓ Spot Size: < 100 nm²
 - ✓ (or smaller for in device testing)
- ✓ Stability: $< 1\%$
- ✓ Long Lifetime

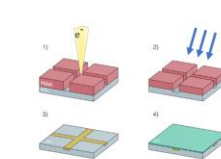
	Units	Schottky TFE	Photo-cathode
ΔE	eV	≥ 0.7	0.3
Temp	K	1800	294
Stability		$< 1\%$	$< 1\%$
I	A / m ²	$\sim 30 \times 10^7$	$> 30 \times 10^7$
Multibeam		> 20	> 20
Cost		Cost prohibited	

Photocathodes have some clear advantages over state-of-the-art electron sources.



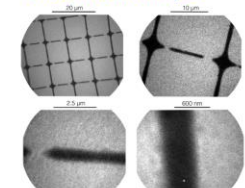
UV-ONEM using LED (275 nm)

1) Create embedded Au nanostructures



2) Cover with photocathode layer: Chromium

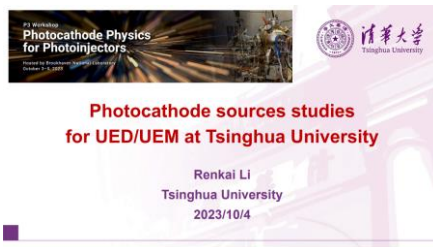
ONEM Proof of Principle!



Illumination time: 10-35 min.
Estimated resolution: 37 nm = $\lambda/7$

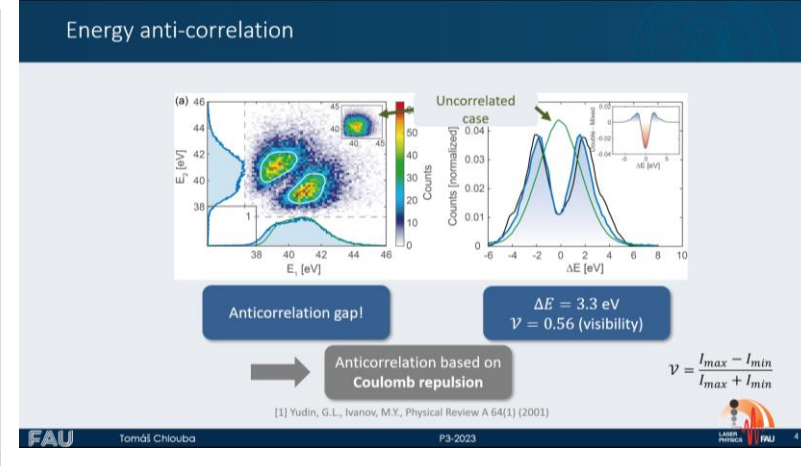
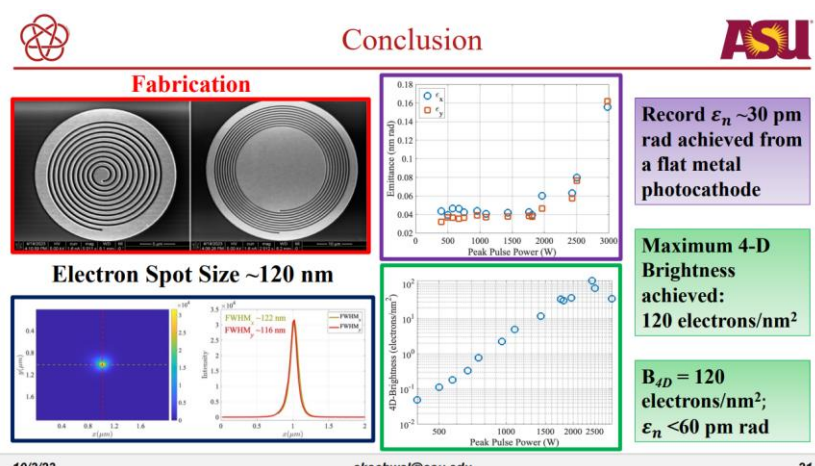
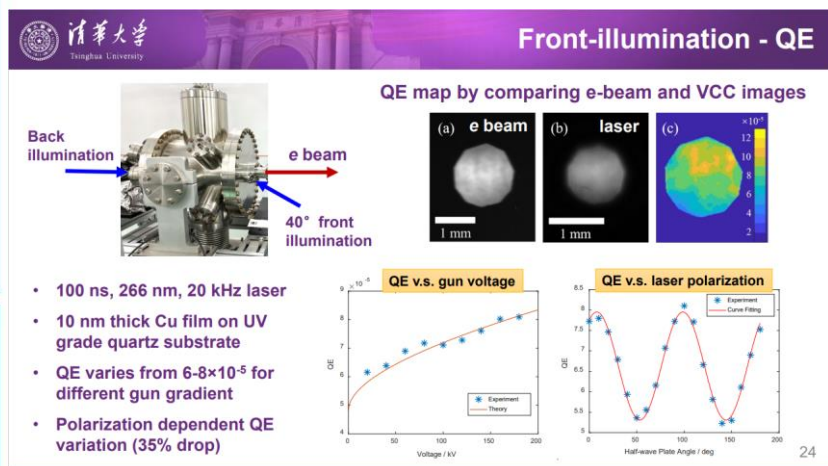
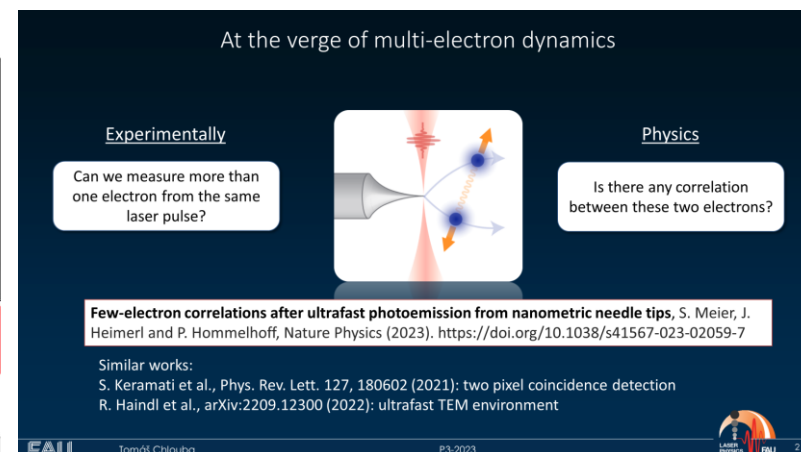
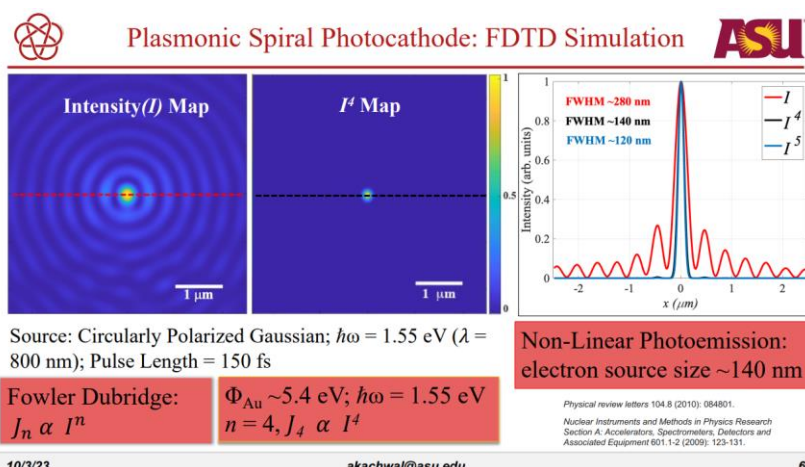
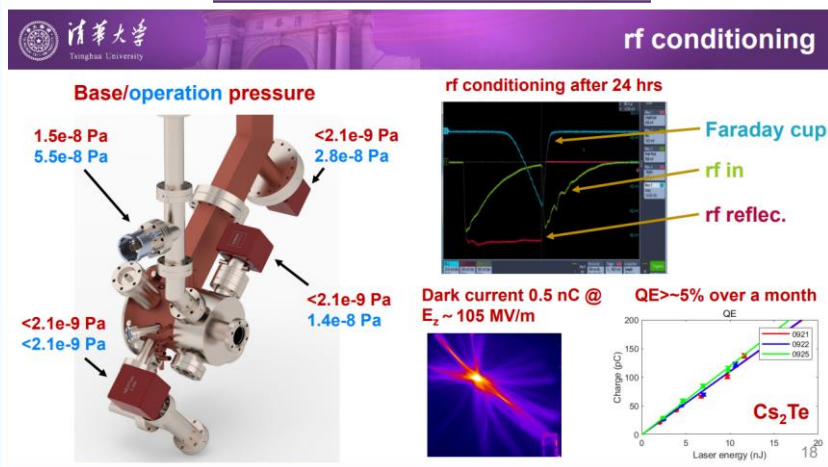
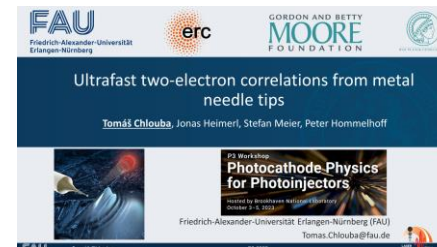


UED/UEM



Bright Electron Beams from Plasmonic Spiral Photocathode

Alimohammed Kachwala
Arizona State University



UED/UEM

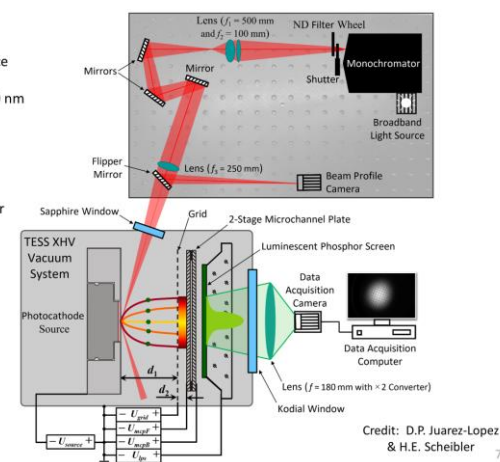


Dr. Lee Jones
Senior Accelerator Physicist
Accelerator Science and Technology Centre
STFC Daresbury Laboratory

TESS: The Transverse Energy Spread Spectrometer
and Recent Experimental Results to Characterise Photocathode Performance

TESS Leading Particulars:

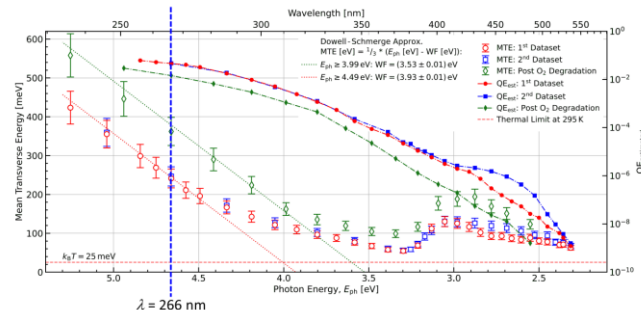
- Laser-driven plasma broadband lightsource
- Twin grating monochromator
 - Usable flux from $\lambda = 236$ nm to > 800 nm
- Filter wheel to avoid space charge
- Beam profile camera at working distance
 - Optimise source spot for each λ
- Sapphire viewport window
 - Maximise UV transmission
- TESS base pressure typically 3×10^{-11} mbar
- LN₂ Cooling loop
- Piezoelectric leak valve for controlled degradation studies
- TESS linked to GaAs PPF at 4×10^{-12} mbar
 - Storage carousel with up to 6 photocathodes
- Vacuum suitcase for sample transfers between systems ($< 1 \times 10^{-10}$ mbar)



L. Jones et al., Rev. Sci. Instrum. 93, 113314 (2022)

Credit: D.P. Juarez-Lopez & H.E. Scheibler

TESS Characterisation of DL CsTe Photocathode (~ 5% QE @ 266 nm)



- MTEs for both datasets broadly agree, and follow Dowell-Schmerge approximation (WF ~ 3.9 eV)
 - O₂ degradation increases MTE (WF ~ 3.5 eV) and reduces estimated QE in comparison to 'clean' surface
- Thermal floor not reached, either for the dominant Cs-Te emitters or the Cs/CsO emitters
- Demonstrates the need for multi-wavelength QE monitor during deposition

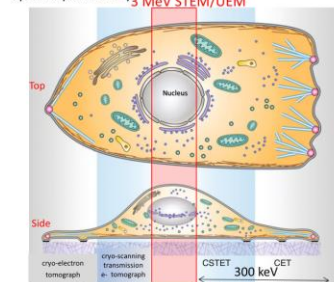
H.M. Hum et al., Proc. IPAC 2023, TUPA030, 1404-1407



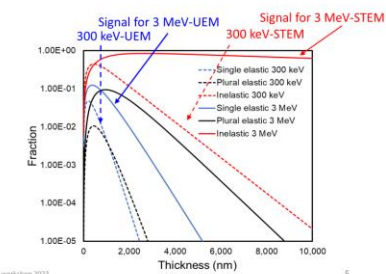
Promise of MeV Microscopy

Benefit of increasing electron energy to MeV

- Life science application:** 3D image intact thick bio-samples studying cell-biology and microbiology in cellular context
 - No need of cryo-FIB (focused ion beam) slicing thick cells
 - Limit to 10-20 lamellae/day, "blindly" select target
 - Speed up discovery
- Why MeV?** Phase contrast (TEM) & amplitude contrast (STEM)
 - 300 keV
 - Single-elastic drop $< 1\%$ after 1- μ m ice layer
 - Inelastic drop $< 1\%$ after 4- μ m
 - 3 MeV
 - Single-elastic drop $< 1\%$ after 2- μ m ice layer
 - Inelastic stays 63% after 10- μ m



Top and side views of a eukaryotic cell. S.G. Wolf, et al., Cellular Imaging, Springer

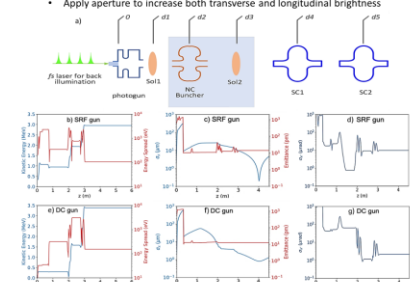


Xi Yang @ P3 workshop 2023

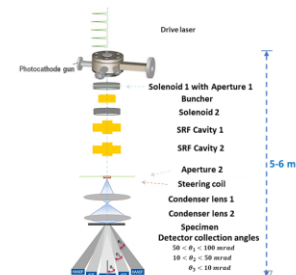
Challenges of implementing MeV STEM

- Reduce beam emittance to ~ 2 μ m with current of 30 – 750 pA
 - Photocathodes & beam dynamics need to improve brightness by > 1000
- Probe size: $\sigma_d = 2$ nm; divergence: $\sigma_\theta \leq 1$ mrad; emittance: $\epsilon_{geo} \leq 2$ μ m

- Reduce laser spot size and MTE from photocathode
- Increase QE $\geq 10^5$
- Beam dynamics come hand in hand with improved emittance
 - Apply aperture to increase both transverse and longitudinal brightness
- Preliminarily MeV-STEM column design (reversal of TEM column)
 - Assume 2 μ m spot at cathode
 - Dose rate 200 to 5k e-/ μ s



J. Maxson and A. Bartnik



Theory

Modeling Optical Interference Effects for Optimization of Electron Emission Properties from Thin Film Semiconductor Photocathodes

D. A. Dimitrov, A. Alexander, C. Huang, N. Moody, V. Pavlenko, E. Simakov, G. Wang, H. Yamaguchi
Los Alamos National Laboratory, Los Alamos, NM 87545, USA
K. L. Jensen,
University of Maryland, College Park, MD 20741, USA
J. Smedley
SLAC National Accelerator Laboratory, Menlo Park, CA 94025, USA
LA-UR-23-31152

D. A. Dimitrov et al., Modeling optical interference effects in thin film semiconductor photocathodes

Optical interference effects in a thin film photocathode

- Light E-field in photocathode:
 $E_{ph}(x) = E_0(t_1 e^{i\kappa_1 x} + r_1 e^{-i\kappa_1 x})$
- The E-field r_i and t_i coefficients depend on indices of refraction $\hat{n}_i = n_i(\omega) + ik_i(\omega)$ in different material layers and on L .
- For normal light incidence, r_i and t_i are derived in K. L. Jensen et al., J. Appl. Phys. **128**, 115301 (2020).

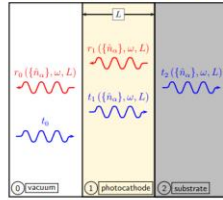


Figure 10: Schematic of incident light on a photocathode thin film of thickness L deposited on a (metal) substrate.

Absorption and transport: thin film photocathode

$$f_{tr}(\omega, E, \cos(\theta)) = \frac{\int_0^L |E_{ph}(x)|^2 e^{-x/(\lambda(E) \cos(\theta))} dx}{\int_0^L |E_{ph}(x)|^2 dx}$$

D. A. Dimitrov et al., Modeling optical interference effects in thin film semiconductor photocathodes

Comparison to QE experimental data (#) from Cs₃Sb on Ag and Si, for $\lambda = 450$ nm and 532 nm.

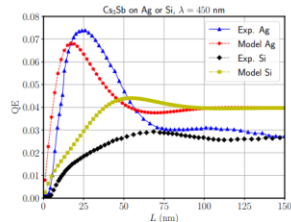


Figure 17: For $\lambda = 450$ nm (2.755 eV), the QE from Cs₃Sb on Ag is highest for Cs₃Sb film thickness near 21 nm.

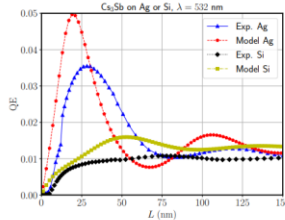
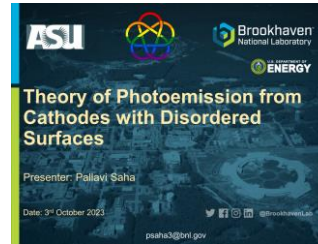


Figure 18: The extended MM for QE shows similar functional behavior with film thickness for both substrates.

D. A. Dimitrov et al., Modeling optical interference effects in thin film semiconductor photocathodes



Expression for QE

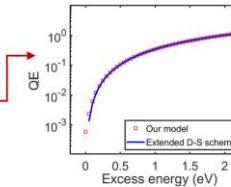


$$\#e^- \text{ emitted} = \int_{-\infty}^{\infty} P_{excitation}(E) P_{transport}(E) P_{emission}(E) dE$$

$$\#e^- \text{ excited} = \int_{-\infty}^{\infty} P_{excitation}(E) dE$$

$$QE(\hbar\omega) = \frac{\#e^- \text{ emitted}}{\#e^- \text{ excited}}$$

Assumption: constant DOS,



Combining Equations (1) through (3),

$$QE(\hbar\omega) = C \frac{\int_{-\infty}^{\infty} D(E) f(E) D(E + \hbar\omega) [1 - f(E + \hbar\omega)] E_{kinetic} dE}{\int_{-\infty}^{\infty} D(E) f(E) D(E + \hbar\omega) [1 - f(E + \hbar\omega)] dE}$$



psaha3@bnl.gov

13



Expression for MTE



$$MTE(\hbar\omega) = \frac{\hbar^2}{2m} \frac{\int_{-\infty}^{\infty} D(E) f(E) D(E + \hbar\omega) [1 - f(E + \hbar\omega)] dE \int_0^{k_{\perp, \max}} 2\pi k_{\perp} k_{\perp}^2 dk_{\perp}}{\int_{-\infty}^{\infty} D(E) f(E) D(E + \hbar\omega) [1 - f(E + \hbar\omega)] dE \int_0^{k_{\perp, \max}} 2\pi k_{\perp} dk_{\perp}}$$

By substituting the value of $k_{\perp, \max}$, where $k_{\perp, \max} = \sqrt{\frac{2m}{\hbar^2} (E_{kinetic})}$

$$MTE(\hbar\omega) = \frac{\hbar^2}{2m} \frac{\int_{-\infty}^{\infty} D(E) f(E) D(E + \hbar\omega) [1 - f(E + \hbar\omega)] E_{kinetic}^2 dE}{\int_{-\infty}^{\infty} D(E) f(E) D(E + \hbar\omega) [1 - f(E + \hbar\omega)] E_{kinetic} dE}$$

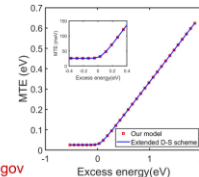
Under the assumption of a constant DOS,

$$MTE = \frac{E_{excess}}{3}, E_{excess} \gg 0$$

$$MTE \rightarrow k_B T, E_{excess} \rightarrow 0$$



psaha3@bnl.gov



14

Photoemission Physics for Photoelectron Spectroscopy (P2) Workshop
Brookhaven National Laboratory, NY, October 3-5, 2023.



Electron Scattering Processes in Photoemission: The Franck-Condon Effect

W. Andreas Schroeder
Louis Angeloni and Ir-Jene Shan
Physics Department, University of Illinois Chicago

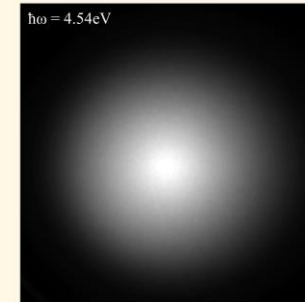
Department of Energy
DE-SC0020387



Metallized diamond(001) emission



$\hbar\omega = 4.54 \text{ eV}$



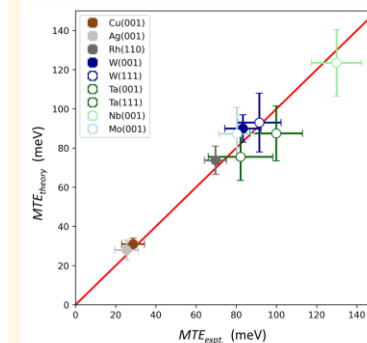
Two emission signals:

- Outer large MTE signal from **strong** optical phonon assisted Franck-Condon effect
 $P_{vac} = P_{band} + n q_{phonon}$
 - Emission of Boltzmann tail of electron distribution from NEA upper CB of diamond ($\chi \approx -1 \text{ eV}$)
 - High emission efficiency over PE barrier due to momentum resonance ($T \rightarrow 1$)
- Inner signal with MTE < 100 meV from electrons **directly** emitted from NEA upper CB of diamond
 - Lower emission efficiency as $P_{vac} \neq P_{band}$; less than ~5% of total signal

BOTH with Gaussian spatial beam profiles

J.D. Rameau et al., Phys. Rev. Lett. **106**, 137602 (2011)

MTE: Theory vs. Experiment



Theoretical MTE:

$$MTE_{theory} = MTE_{e-e} + MTE_{band}$$

$$\dots MTE_{band} \geq \left(\frac{m_T^*}{m_0}\right) k_B T_e; m_T^* < m_0$$

$$MTE_{band} \leq 1.5 k_B T_e; m_T^* > m_0$$

Emission processes **not** independent:
BOTH emissions from virtual excited band states

\Rightarrow Convolution in momentum space
 \therefore Addition of p_T variances (i.e., MTEs)

\dots Consistent with observation of a **single** Gaussian electron beam profile

D. A. Dimitrov et al., Modeling optical interference effects in thin film semiconductor photocathodes

Theory

FAU GORDON AND BETTY MOORE FOUNDATION

Tracing attosecond dynamics of electron emission from metallic nanotip

Tomáš Chlouba, Philip Dienzbier, Lennart Seifert, Timo Paschen, Andreas Liehl, Alfred Leitenstorfer, Thomas Fennel and Peter Hommelhoff

23 Workshop Photocathode Physics for Photoinjectors

Research Alexander von Humboldt Stiftung

www.leidos-fau.de

FAU Tomáš Chlouba P3-2023

A Delta Barrier in a Well And Its Generalization For Emission Studies

leidos U.S. NAVAL RESEARCH LABORATORY TOWSON UNIVERSITY

Kevin Jensen*, Jeanne M. Riggs*, Andrew Shabaev*, Michael Crotley*, Joseph Prestigiacomo*, John Petillo*, London, Maryland, USA, *Naval Research Laboratory, Washington, DC, *Towson University, MD

Day 2 - 1:55-2:20 PM Wednesday Oct 4, 2023
Photocathode Physics for Photoinjectors Workshop 2023
Oct. 2-5, 2023 Charles B. Wang Center (Story Brook University)

DISTRIBUTION STATEMENT A: Approved for public release; distribution is unlimited

P3 2023
2023 Photocathode Physics for Photoinjectors Workshop
Brookhaven National Laboratory
3-5 October 2023

Theory Session

Beam Transport Parameter Sensitivity Using Adjoint Methods for 2D Axisymmetric Systems in Static Fields with MICHELLE

John Petillo, Eugene Ostashev, Aaron Jensen, Andrew Shabaev, Brian Bracken, Dennis Kozlovskii, et al. (in progress)

This work was supported by Navy contract N68339-22-C-0004 and Leidos IR&D

Distribution A: Approved for Release. Distribution is unlimited

leidos

How about attosecond precision physics at the surface of a solid?

1560 nm 780 nm

Yield (ϕ_{rel}) Energy (ϕ_{rel})

e^- -trajectory

• $\omega - 2\omega$ field with variable relative phase

• Needle tip (gold, tungsten) with radius of curvature $\sim 10 - 40$ nm

• Nearfield intensities $10^{11} - 10^{13}$ W/cm²

FAU Tomáš Chlouba P3-2023

leidos AFRL U. Towson

Introduction Eigenvalues Simulations Background Delta Function Model Modification to Delta Model

BACKGROUND

(a) nanodiode simulation (b) photoemission from needle (c) Nanoscale Si FEA (d) quantized nano-object (e) Nano-vacuum channel transistor

FIG. S17: Energy band diagram of tunneling barrier with a quantum dot

V > 200 V

DISTRIBUTION STATEMENT A: Approved for public release; distribution is unlimited

A Delta Barrier in a Well And Its Generalization For Emission Studies

cy 3 of 17

Adjoint Method Background: Sensitivity Function

Basic question: How do small changes in position or potential of anode affect the properties of the beam leaving the gun?

Focus Electrode Cathode Anode Beam Exit

Conventional solution: Trial and error. Do many simulations with different anode potentials or positions to understand sensitivities. Also leads to selecting the best (optimized) solution based on some performance metric.

DYMNISO Distribution A: Approved for Release. Distribution is unlimited

leidos

Acceleration with Alternating phase focusing

T. Chlouba*, R. Shalun*, S. Kraus*, L. Brückner*, J. Litzel, P. Hommelhoff, Coherent Nanophotonic Electron Accelerator, Nature (2023), in press.

(a) $\Delta\varphi = 120^\circ$ (b) $\Delta\varphi = 240^\circ$

(c) Defocusing (d) Focusing (e) Defocusing

40.7 keV 20.4 keV

FAU Tomáš Chlouba P3-2023

leidos AFRL U. Towson

Introduction Eigenvalues Simulations Time Evolution Quantum Potential Density in Split Well

EXACT EVOLUTION OF EIGENSTATES

(a) $n = 1; t_{\text{max}} = 375$ (b) $n = 1; t_{\text{max}} = 375$

Time evolution of probability density using solid curve $\psi_n(k); \epsilon = 0.3$

Time evolution of probability density using dashed curve $\psi_n(k); \epsilon = 0.2$

DISTRIBUTION STATEMENT A: Approved for public release; distribution is unlimited

A Delta Barrier in a Well And Its Generalization For Emission Studies

cy 14 of 17

Mean Displacement: 2D Axisymmetric Electron Gun - Manufacturing sensitivity to AK-Gap axial offset

No-B

Results:

- The test case where the direct perturbation of a voltage change worked as expected.
- The reverse-beam case was oddly sensitive to changes.

Reverse case ran smoothly

DYMNISO Distribution A: Approved for Release. Distribution is unlimited

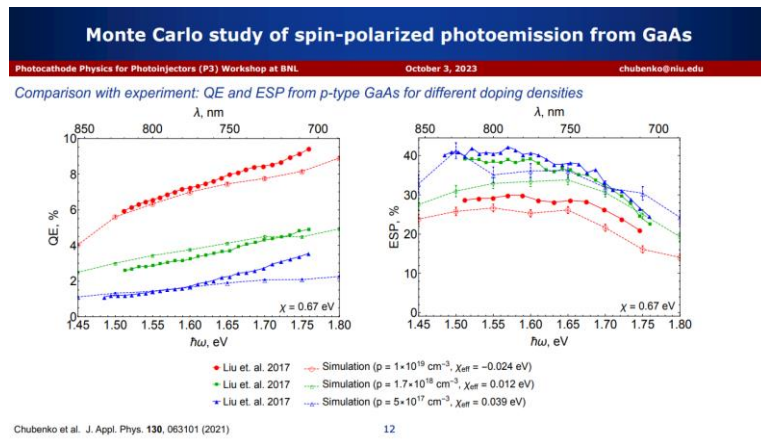
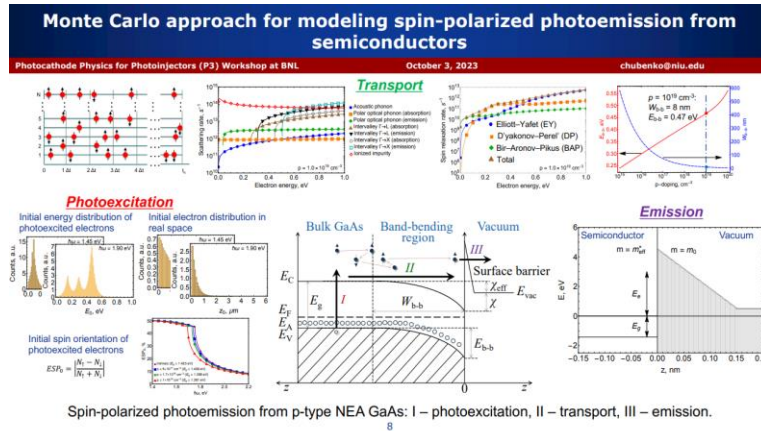
leidos

Spin polarized

Northern Illinois University

Monte Carlo Modeling of Spin-Polarized Photoemission

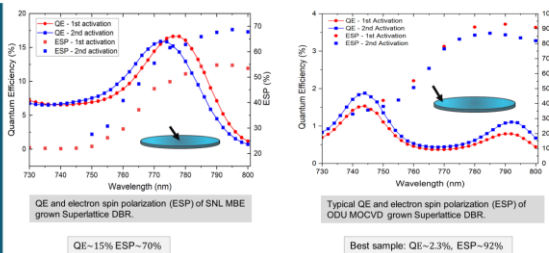
Oksana Chubenko
Department of Physics, Northern Illinois University, DeKalb, IL 60115



Recent Advances in Superlattice GaAs/GaAsP Photocathodes for Spin-Polarized Electron Sources

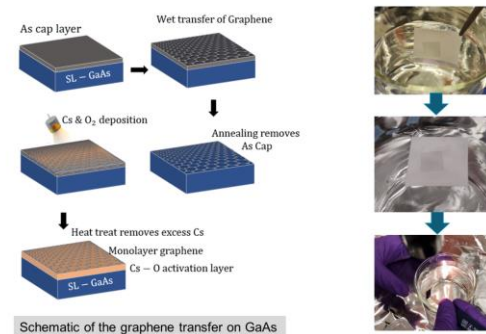
Jyoti Biswas
On behalf of the collaborator
Electron Ion Collider, BNL

GaAs/GaAsP superlattice DBR: QE, ESP



J. Biswas et al. AIP Advances 13, 085106 (2023); <https://doi.org/10.1063/1.519183>

Transfer of Graphene onto GaAs



Inspired by our previous work on Cesium intercalation of graphene: Biswas et al. APL Mater. 10, 111115 (2022)

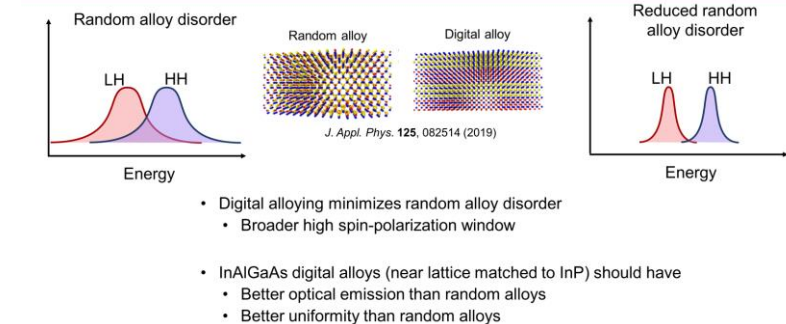
Strained superlattice InAlGaAs/AlGaAs spin-polarized photocathodes implemented with both random and digital alloying

Aaron Engel¹, Marcy Stutzman², Jason Dong¹, Christopher Palmstrom^{1,3}

¹Materials Dept., University of California, Santa Barbara
²Center for Injections and Sources, Thomas Jefferson National Accelerator Facility
³Dept. of Electrical & Comp. Eng., University of California, Santa Barbara



Approach to reduce alloy disorder and improve uniformity



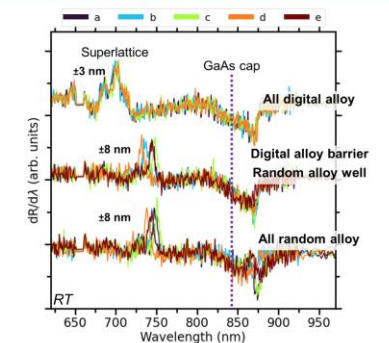
D. Song, Y.T. Lee, J. Cryst. Growth 270, 295 (2004)
I. J. Fritz, J. F. Klem, M. J. Hafich, A. J. Howard Appl. Phys. Lett. 66, 2825 (1995)
C.S. Wang, A.C. Gossard, L.A. Coldren J. Cryst. Growth 277, 13 (2005)

Digital alloys improve uniformity for cavity resonance

- Uniformity problematic in the past
 - Essential for resonant cavity with DBR
- Broader features in digital alloy well
- Digital alloy well + barrier makes significant improvement to uniformity



Uniformity is adequate... now DBRs



Spin polarized



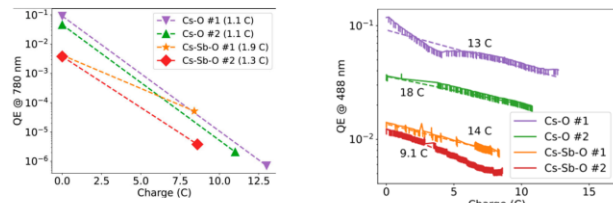
Cornell Laboratory for
Accelerator-based Sciences
and Education (CLASSE)

Polarized Photocathodes for Future Applications

Samuel J. Levenson
Photocathode Physics for Photoinjectors Workshop
Stony Brook, NY, USA
October 5, 2023

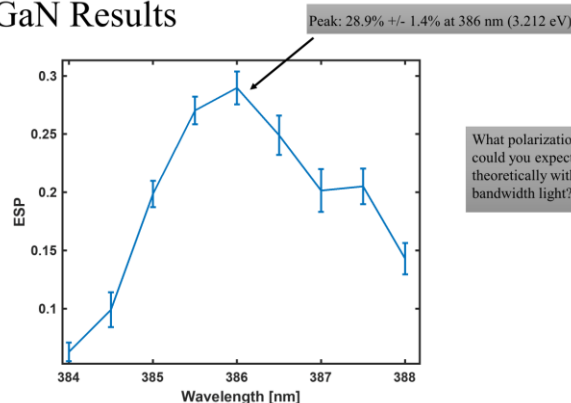
Alternative NEA Coatings: Cs-Sb-O High current studies in the HERACLES beamline

- No improvement in the charge lifetime at 488 nm, modest improvement at 780 nm
 - Sb improves chemical poisoning, ion back bombardment less so
 - Relative QE change smaller for Cs-Sb-O samples
- Now, we want to optimize the thicknesses of these activation layers w.r.t. operational lifetime
Current project: HERACLES runs with varying activation layer thicknesses

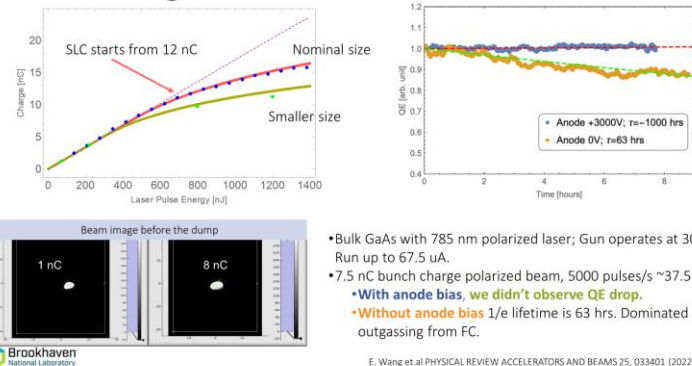


J. K. Bae, M. Andorf, A. Bartnik, A. Galdi, L. Cultrera,
J. Masson and I. Bazarov, *AIP Adv.*, 2022, 12, 095017.

Cubic GaN Results



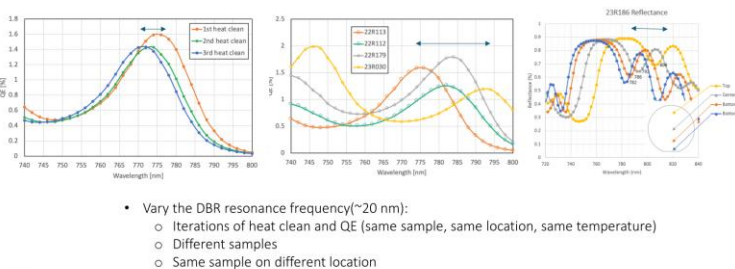
Bunch Charge and Cathode Lifetime



E. Wang et al *PHYSICAL REVIEW ACCELERATORS AND BEAMS* 25, 033401 (2022)

Third figure is provided by A. Master

DBR samples resonance frequency variation



Atomic Layer Deposition (ALD) - An Enabler for Photocathodes?

Harish Bhandari, Director for Advanced Thin Films Technologies
hbhandari@rmdinc.com



Strained Layer Epitaxy CdTe/ZnTe

Cd _{1-x} Zn _x Te	Lattice Parameter (Å)	% Strain
x=0 (CdTe)	6.48	0.00
x=0.1	6.451	0.45
x=0.2	6.422	0.90
x=0.3	6.371	1.68
x=0.4	6.298	2.81
x=0.5	6.25	3.55
x=0.6	6.218	4.04
x=0.7	6.183	4.58
x=0.8	6.128	5.43
x=0.9	6.051	6.62
x=1 (ZnTe)	6.1	5.86

Preliminary investigation for CdTe indicate:

- 1.5eV bandgap permits excitation at 780nm;
- ~2% strain has the necessary valence band splitting (0.1eV) to realize 100% polarization;
- p-type can be achieved with antimony/arsenic doping;
- has excellent absorption and spin relaxation time;
- negative electron affinity has been demonstrated with Cs-O surface treatments.

What is needed:

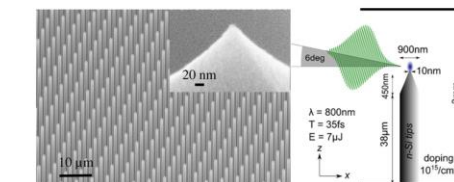
- DFT calculations of band structure
- Monte Carlo simulations of transport properties



UNCLASSIFIED

rmd.dynasil.com | 13

GaAs Nanotip Activation



- ALD can be used for nanotip activation
- RMD does have a proprietary Cs ALD precursor (metal organic)
- On-site Cs₂O surface activation is possible

Swanwick, Michael E., et al. "Nanostructured ultrafast silicon-tip optical field-emitter arrays." *Nano letters* 14.9 (2014): 5035-5043.



UNCLASSIFIED

rmd.dynasil.com | 14 of

P3 2025: Welcome to the Desert



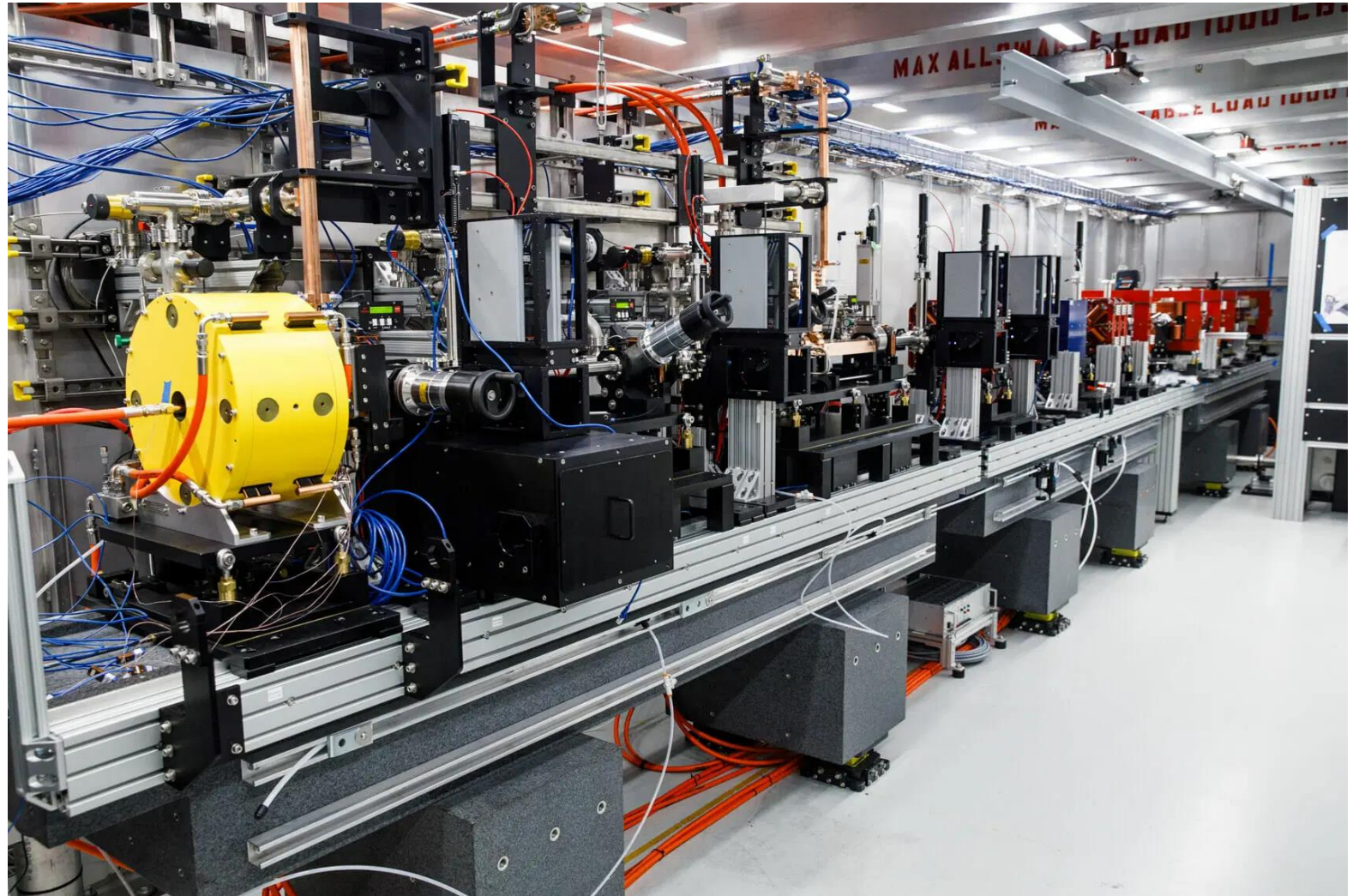
Beus CXFEL Lab



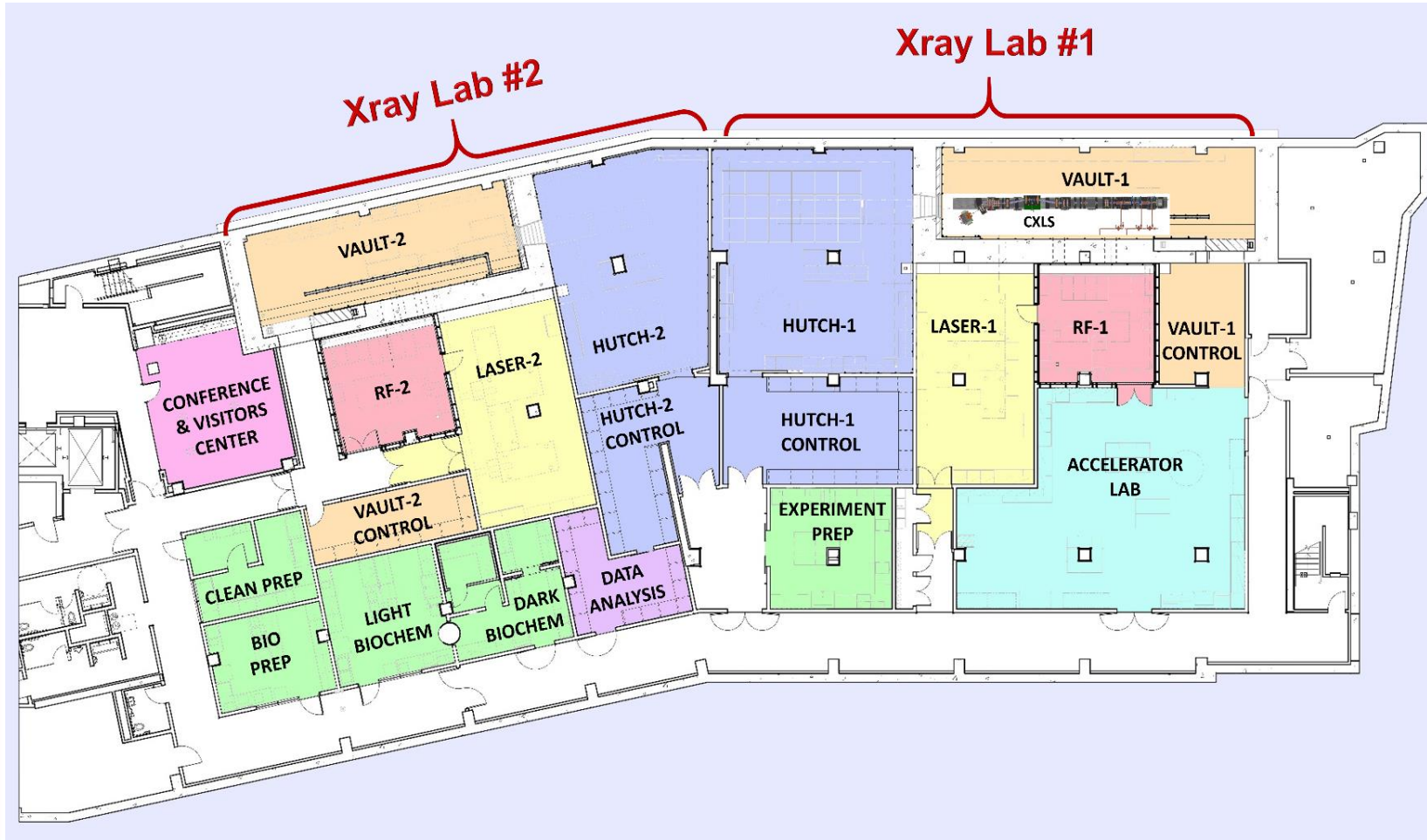
10 MeV linac based
Incoherent Compton X-ray
source – first x-rays

\$90M NSF X-ray facility

Coherent X-ray Compton
source research



Beus CXFEL Lab



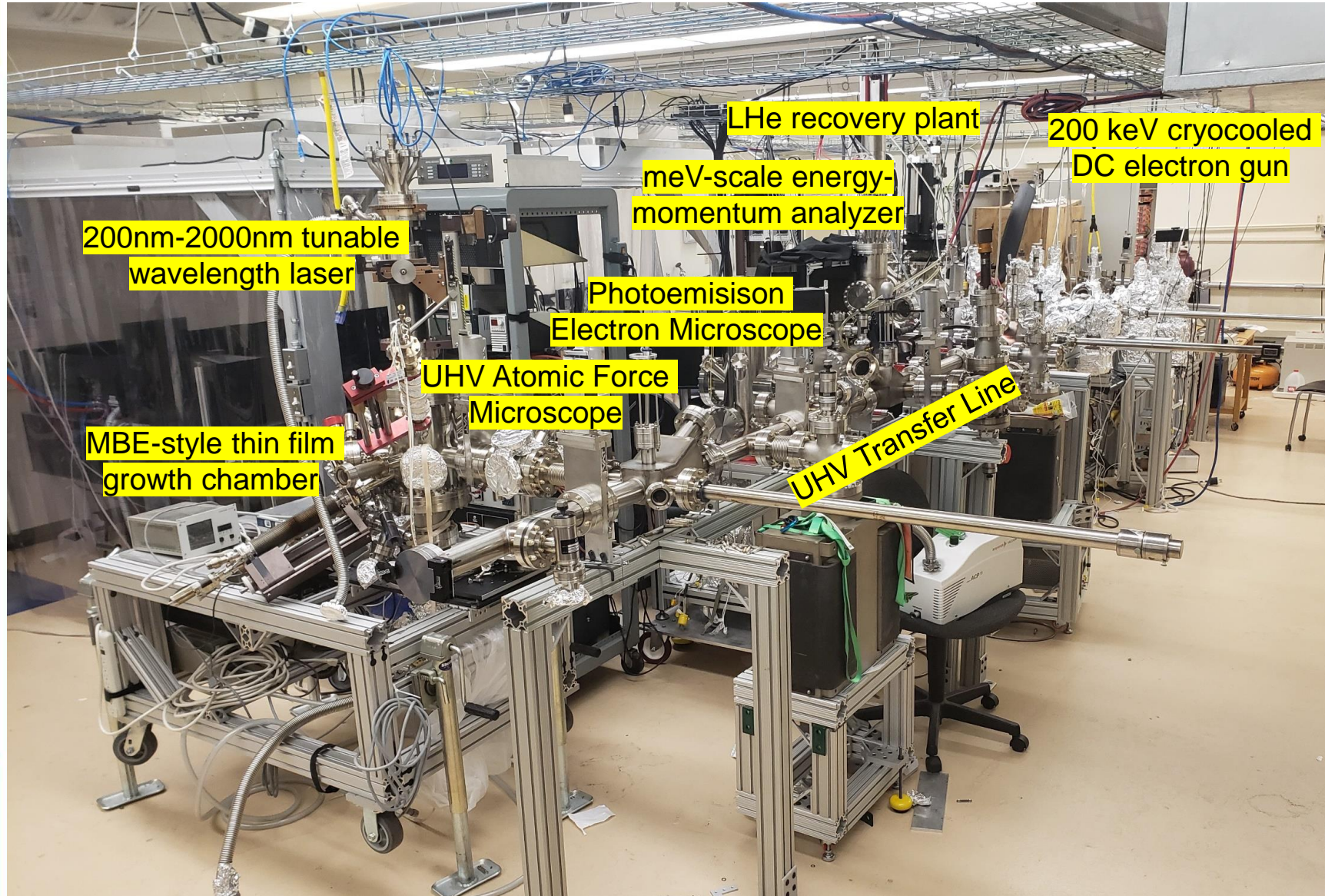
Unique ultra-stable
photoinjector facility

2 vaults:

- Vibration free
- EM free
- Radiation shielded

Large Dedicated X-ray
'hutches' + prep labs

Photoemission and Bright Beams Lab



UHV thin film growth

Atomic scale surface characterization

Fundamental photoemission physics

Electron Beam Physics

Ultrafast Electron Diffraction (soon)

John M. Cowley Center for High Resolution Electron Microscopy

Nion UltraSTEM100



Sub-Å spatial resolution
Sub-10 meV energy spread

JEOL ARM200F



FEI Titan 80-300



- Vibrational Spectroscopy in EM
- Aloof EM
- Lorentz EM ...

Nanofab and Eyring Materials Center



Large University Campus

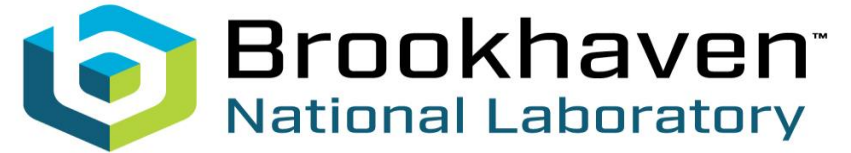
- Strong expertise in nanoscience and ultrafast physics and upcoming accelerator physics
- >60,000 students



P3 2025: See you next year

But will it still be P3...?





Thank you!!!

Thanks to all authors from which I have taken slides and to Siddharth Karkare who provided information on next P3 workshop at ASU

Supported by DE-SC00012704

